# Global geometry of a spherically symmetric universe

V. A. Berezin, V. A. Kuz'min, and I. I. Tkachev

*Institute for Nuclear Research, Academy of Sciences of the USSR*

A full classification is given of the mutual disposition of $R$ and $T$ regions of space-time as a function of the structure of the energy-momentum tensor. The geometry corresponding to the chaotic inflation scenario is discussed.

## 1. INTRODUCTION

The question of the origin of the universe and of the first few moments of its development is intimately related to the topology and global geometry of the corresponding space-time manifold. In its general form, this problem is unusually complicated and multifaceted. In particular, it is important to know the structure of infinities, horizons, and singularities. The subdivision of space into $R$ and $T$ regions is also important. In this paper, we shall confine our attention to spherically symmetric spaces, and obtain a number of completely general relationships that limit the possible structure of space-time. In particular, we shall find all the possible variants of the mutual disposition of the $R$ and $T$ regions, and the relationship between a given disposition and the structure of the energy-momentum tensor.

It was recently shown[1,2] that the existence of inflating fluctuations in the chaotic inflation scenario[3] was frequently due to a "molehill"-type singularity (or, as it is still called, a "white hole"). We shall examine possible limitations imposed by the $R$ and $T$ classification on the initial case of the universe in this scenario (an inflating fluctuation is always related to the existence of a $T_+$ region of space-time). All we find is that the existence of such $T_+$ regions is due to an initial singularity, but we do not determine its type (although we admit, say, a Friedman singularity). However, the final answer will have to await a more informative analysis, similar to that carried out in Ref. 1 (unfortunately, Ref. 1 was essentially confined to a comprehensive analysis of the pure vacuum case in the thin-wall approximation).

## 2. SPHERICALLY SYMMETRIC SPACE-TIME

The interval between closely spaced points in the case of spherical symmetry can be written in the form

$$ds^2 = g_{00}dt^2 + 2g_{01}dtdq + g_{11}dq^2 - r^2d\Omega^2, \tag{1}$$

where

$$d\Omega^2 = d\theta^2 + \sin^2\theta \, d\varphi^2,$$

and $g_{00}, g_{01}, g_{11}$, and $r$ are functions of only the two variables $q$ and $t$. In the metric given by (1), we can transform to the new variables $\tilde{q} = \tilde{q}(t, q)$ and $\tilde{t} = \tilde{t}(t, q)$ in such a way that this transformation does not involve angle variables. Consequently, two coordinate conditions can be imposed without loss of generality. One of them can be taken to be the orthogonality condition $g_{0+} = 0$. The metric then assumes the form

$$ds^2 = e^\nu dt^2 - e^\lambda dq^2 - r^2(q, t)d\Omega^2. \tag{2}$$

We shall choose the coordinate $q$ so that it increases during motion from the chosen center outward.

### 1. The $R$ and $T$ regions of space-time: definitions

Curved space-time can be divided into parts ($R$ and $T$ regions[4]) that differ fundamentally in the way test particles behave within them. This partition arises because the vector normal $N_\mu \equiv r_{,\mu}$ to the surface $r = $ const can be either spacelike or timelike. In the former case, the quantity

$$\Delta \equiv g^{\alpha\beta}r_{,\alpha}r_{,\beta} \tag{3}$$

is negative, $\Delta < 0$, and the corresponding region is called the $R$ region (in flat space-time, the $R$ region completely occupies the entire manifold). In the second case we have $\Delta > 0$. This is referred to as the $T$ region. In the coordinate system (2) that we have chosen, we have

$$\Delta = e^{-\nu}\dot{r}^2 - e^{-\lambda}r'^2. \tag{4}$$

Since $\Delta > 0$ holds in the $T$ region, the condition $\dot{r} = 0$ cannot be satisfied, i.e., the conditions $\dot{r} > 0$ and $\dot{r} < 0$ are invariant under continuous coordinate transformations in the $T$ region. The region where $\dot{r} > 0$ holds will be referred to as the expansion $T$ region (or $T_+$ region), whereas the region where $\dot{r} < 0$ holds will be called the contraction $T$ region (or $T_-$ region). We shall define $R_+$ as the region with $r' > 0$ and $R_-$ as the region with $r' < 0$. In the $R$ region, an observer located on an $r = $ const surface can dispatch two light rays along the radius: one in the inward direction and the other in the outward direction relative to the surface. Since, in the $T$ region, the $r = $ const surface is spacelike, the two outgoing radial light rays lie on either side of it (looking ahead, we recommend examination of Fig. 1). Consequently, any material object can cross the given $r = $ const surface only once in the $T$ region. Because of this, the definition of the $T_-$ region ($T_+$ region) is also related to the existence of trapping (antitrapping) surfaces.

The above definitions are summarized in the Table. It turns out that the $R$ and $T$ regions cannot be disposed of relative to one another in an arbitrary manner in space-time. However, before we proceed to the examination of this ques-

TABLE I.

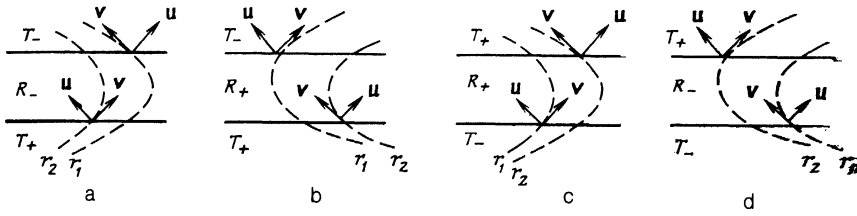| $R_+$ | $R_-$ | $T_+$ | $T_-$ |
|---|---|---|---|
| $\Delta < 0$ | | $\Delta > 0$ | |
| $r' > 0$ | $r' < 0$ | $\dot{r} > 0$ | $\dot{r} < 0$ |

FIG. 1. Space-like boundary between $R$ and $T$ regions: (a) and (b) correspond to $\beta > 0$, and (c) and (d) to $\beta < 0$.

tion, we must write down the Einstein equations in a form convenient for subsequent use.

## 2. Einstein equations for spherically symmetric metric

The Einstein equations in the metric given by (2) have the form[5]

$$-e^{-\lambda}\left(2\frac{r''}{r}+\frac{r'^2}{r^2}-\frac{r'\lambda'}{r}\right)+e^{-\nu}\left(\frac{\dot{r}\dot{\lambda}}{r}+\frac{\dot{r}^2}{r^2}\right)+\frac{1}{r^2}=8\pi\varkappa T_0{}^0,$$

$$-e^{-\lambda}\left(\frac{\nu'r'}{r}+\frac{r'^2}{r^2}\right)+e^{-\nu}\left(2\frac{\ddot{r}}{r}+\frac{\dot{r}^2}{r^2}-\frac{\dot{r}\nu}{r}\right)+\frac{1}{r^2}=8\pi\varkappa T_1{}^1,$$

$$\left(-2\frac{\dot{r}'}{r}+\frac{r'\dot{\lambda}}{r}+\frac{\dot{r}\nu'}{r}\right)=8\pi\varkappa T_{01},$$

$$-e^{-\lambda}\left(\frac{\nu''}{2}+\frac{\nu'^2}{4}+\frac{r''}{r}-\frac{r'\lambda'}{2}+\frac{r'\nu'}{2}-\frac{\nu'\lambda'}{4}\right)$$

$$+e^{-\nu}\left(\frac{\ddot{\lambda}}{2}+\frac{\dot{\lambda}^2}{4}+\frac{\ddot{r}}{r}-\frac{\dot{r}\nu}{2}+\frac{\dot{r}\dot{\lambda}}{2}-\frac{\dot{\nu}\dot{\lambda}}{4}\right)=8\pi\varkappa T_2{}^2=8\pi\varkappa T_3{}^3.$$

Multiplying the first equation by $r^2r'$ and the second by $(-e^{-\nu}r^2\dot{r})$, and adding, we obtain

$$e^{-\nu}(2r\dot{r}'\dot{r}-r\dot{r}^2\nu'+\dot{r}^2r')-e^{-\lambda}(2rr''r'+r'^3-rr'^2\lambda')+r'$$

$$=8\pi\varkappa r^2[T_0{}^0r'-T_1{}^0\dot{r}] \tag{6}$$

which can be written in the form

$$[r(1+\Delta)]'=8\pi\varkappa r^2[(T_0{}^0+T_1{}^1)r'-T_1{}^0\dot{r}-T_1{}^1r']. \tag{7}$$

Similarly, multiplying the second equation by $r^2\dot{r}$ and the third by $e^{-\lambda}r^2r'$ and adding, we obtain

$$[r(1+\Delta)]^\cdot=8\pi\varkappa r^2[(T_0{}^0+T_1{}^1)\dot{r}-T_0{}^0\dot{r}-T_0{}^1r']. \tag{8}$$

Equations (7) and (8) can be combined into the single vector equation that we require:

$$[r(1+\Delta)]_{,\mu}=8\pi\varkappa r^3[Tr_{,\mu}-T_\mu{}^\nu r_{,\nu}] \tag{9}$$
$$(\mu,\ \nu=0,\ 1),\qquad T\equiv T_0{}^0+T_1{}^1.$$

We note that, in the case of spherical symmetry, the components $T_2^2 = T_3^3$ are invariants of the transformations $\tilde{t} = \tilde{t}(t, q), \tilde{q} = \tilde{q}(t, q)$. Consequently, the sum $T = T_0^0 + T_1^1$ is also an invariant.

This vector equation (equivalent to two scalar equations) must be augmented by the conservation equation (10)

$$T_\mu{}^\nu{}_{;\nu}=0, \tag{10}$$

where the semicolon represents the covariant derivative with respect to the complete four-dimensional metric (2). It cna be shown that the two equations in (9) and the two in (10) constitute a set of equations that is equivalent to the set of four Einstein equations for a spherically symmetric metric [the proof of this relies on the integrability of the system (9)].

## 3. GLOBAL GEOMETRY OF SPHERICALLY SYMMETRIC SPACE

We must now determine the different mutual dispositions of the $R$ and $T$ regions in space-time that constitute the solution of the Einstein equations. The surface separating these two regions (we shall represent it by the symbol $\Sigma$) is defined by the equation $\Delta = 0$ and can be spacelike, timelike, or isotropic. We shall investigate all three cases. Our strategy will be as follows. We shall send test light rays from the surface to establish the sign of $\Delta$ in the neighborhood of $\Sigma$. This means that our analysis will be most conveniently expressed in terms of isotropic coordinates. An arbitrary spherically-symmetric metric can be written in terms of these coordinates in the form

$$ds^2=2H(u,\ v)dudv-r^2(u,\ v)d\Omega^2. \tag{11}$$

We shall choose the coordinates $u$ and $v$ so that they will be directed into the future. In the signature $(+, -, -, -)$, we then have $H > 0$. Equation (3) yields the equation of the surface $\Sigma$:

$$\Delta=H^{-1}r_{,u}r_{,v}=0. \tag{12}$$

Hence, it follows that we can choose the coordinate $v$ so that the following condition is satisfied on $\Sigma$:

$$r_{,v}=0, \tag{13}$$

i.e., either the lines of constant $r$ cut the surface $\Sigma$ in the same way as a ray of light (at 90° on the Penrose diagram), or the $\Sigma$ and $r = $ const surfaces coincide, since they are isotropic.

On the $\Delta = 0$ surface, the components $u$ and $v$ of the Einstein equations (9) assume the form

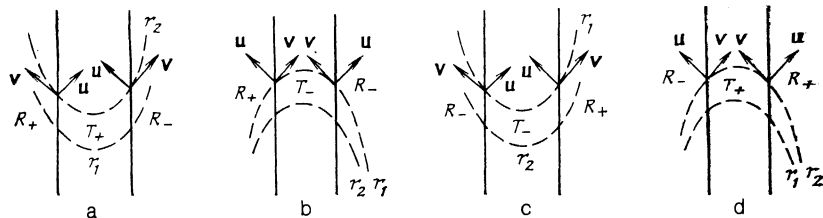$$r\Delta_u=(8\pi\varkappa r^2 T_v{}^v-1)r_u, \tag{14a}$$



FIG. 2. Timelike boundary between $R$ and $T$ regions: (a) and (b) correspond to $\beta > 0$, and (c) and (d) to $\beta < 0$.

$$r\Delta_v = -8\pi\varkappa r^2 T_v{}^u r_u. \tag{14b}$$

The vector normal on the surface $\Sigma$ has the components $N_\mu = \Delta_{,\mu}$. We now introduce the invariant

$$\Delta_3 \equiv \Delta_{,\mu}\Delta_{,\nu}g^{\mu\nu} \tag{15}$$

and the notation

$$\alpha \equiv \mathrm{sign}\,(8\pi\varkappa r^2 T_v{}^v - 1), \qquad \beta \equiv \mathrm{sign}\,T_v{}^u. \tag{16}$$

In that case, sign $\Delta_3 = -\alpha\beta$ and, for $\alpha\beta > 0$, the surface $\Sigma$ is timelike whereas for $\alpha\beta < 0$ it is spacelike; when $\Sigma$ is isotropic, we have either $\alpha = 0$ or $\beta = 0$.

The sign of the $T$ region is uniquely related to sign $r_{,u}$. Let us suppose that sign $r_u = p$; it then follows from the condition that the vector $r_u$ lies in the $T$ region that it also lies in the $T_p$ region because the coordinates $u$ and $v$ increase in the direction of increasing time. On the boundary of the $R$ and $T$ regions, on the other hand, this means that the vector $r_u$ either enters or leaves the $T_p$ region. Henceforth, we shall also use the following relationships that result from (14):

$$\mathrm{sign}\,\Delta_u = \alpha\,\mathrm{sign}\,r_u, \qquad \mathrm{sign}\,\Delta_v = -\beta\,\mathrm{sign}\,r_u. \tag{17}$$

We now turn to a systematic analysis of the resulting possibilities.

## 1. Spacelike surface $\Sigma$ (i.e., $\alpha\beta < 0$)

*1.1. Suppose that $\beta > 0$ (and, consequently, $\alpha < 0$).* Thus, we shall agree that, on all the diagrams we take the time axis upward and the coordinate $q$ axis to the right. In the case of the spacelike surface $\Sigma$, this will mean that the $T$ region can lie either above or below the $R$ region. Suppose that the $T$ region lies above the $R$ region. Then, since $\Delta > 0$ in the $T$ rgion, we have $\Delta < 0$ in the $R$ region, and we conclude that sign $\Delta_u = \mathrm{sign}\,\Delta_v > 0$ on the surface $\Sigma$. From (17) we now find that sign $r_u < 0$, and the $T$ region is a $T_-$ region. Similarly, we find that the $T$ region lying above the $R$ region is a $T_+$ region. The sign of the $R$ region in both these cases is undetermined and can be arbitrary. The corresponding mutual disposition of the $R$ and $T$ regions is shown in Figs. 1a and b.

*1.2. $\beta < 0$.* All the possible situations corresponding to this case will be obtained by replacing $T_p$ with $T_{-p}$ throughout Figs. 1a and b. The convexity of the $r = \mathrm{const}$ lines is then replaced with the opposite convexity. The result is shown in Figs. 1c and d.

## 2. Timelike surface $\Sigma$ ($\alpha\beta > 0$)

*2.1. $\beta > 0$ (and, consequently, $\alpha > 0$).* The $T$ region can now lie on the right or on the left of the $R$ region. Suppose that the $T_+$ region lies on the right. We then have sign $\Delta_u = +1$, sign $\Delta_v = -1$ [see (17)] and, since $d\Delta > 0$ as we move from $R$ into $T$, it is clear that the $u$ line is directed into the $T$ region and the $v$ line into the $R$ region (see Fig. 2a). Next, the $T_+$ region corresponds to $r_1 < r_2$, so that $R_+$ lies to the left of $T_+$. Similar reasoning applied to the possible disposition of the $T_+$, $T_-$ regions leads to the conclusion that, when $\beta > 0$, only the situations shown in Figs. 2a and b are possible.

*2.2. $\beta < 0$.* All the possible dispositions of $R$ and $T$ regions for $\beta < 0$, $\alpha\beta > 0$ can be found by replacing $R_p$ with $R_{-p}$. The convexity of the $r = \mathrm{const}$ lines is then reversed; see Figs. 2c and d.

## 3. Isotropic surface $\Sigma$

*3.1. $\alpha\beta = 0$, $\beta > 0$.* From Eq. (14a), we find that $\Delta_u = 0$. Consequently, the $u$ line points along the $\Delta = 0$ surface and the direction of the $v$ line is determined unambiguously. Repeating the discussion given in Sec. 2.1, we find all the possible mutual dispositions of $R$ and $T$ regions. They are shown in Fig. 3a. We emphasize that, actually, we have obtained only the local form of the boundary between $R$ and $T$ regions. Figure 3 collects together all the possible combinations in a maximally extended configuration (in which the conditions of Sec. 3.1 remain in force throughout). The Penrose diagram of a real metric can contain only certain subblocks of Fig. 3 (see later). This reservation applies to all the diagrams in Sec. 1–3.

*3.2. $\alpha\beta = 0$, $\beta < 0$.* The corresponding diagram is shown in Fig. 3b.

*3.3. $\alpha\beta = 0$, $\alpha > 0$.* It follows from (14b) that $\Delta_v = 0$. Since $r_v = 0$ as well, we find that, in this case, the $v$ points simultaneously along the $\Delta = 0$ and $r = r_0 = \mathrm{const}$ surfaces. Consequently, by definition, the $\Delta = 0$ surface must be the event horizon, i.e., an isotropic surface that does not run to $r = \infty$. Hence, the $r = \mathrm{const}$ surfaces now do not cut the surface $\Delta = 0$. However, the function $r_u$ must be continuous throughout (since, otherwise, we would have a singular surface and $r_{uu}$ would appear in the Einstein equations). Hence, it follows that, if the radii increase along $u$ in the $T$ region ($T_+$ region), they will continue to increase in the $R$ region near the boundary. If we now repeat the reasoning given in the last Sections, we find the possible dispositions of the $R$ and $T$ regions. They are shown in Figs. 3c and d for different signs of $\alpha$.

Summarizing Sec. 3, we note that the $\alpha > 0$ diagram is obtained from the $\beta > 0$ diagram by replacing $R_p$ with $T_{-p}$ and reversing the direction of convexity of the $r = \mathrm{const}$ lines. This also applies to the $\alpha < 0$, $\beta < 0$ diagrams.

## 4. EXAMPLE. SYSTEM CONSISTING OF A SCALAR FIELD AND AN IDEAL FLUID

We shall now apply the classification developed above to the important case of a system consisting of a mixture of a scalar field and an ideal fluid. The energy-momentum tensor for a system of this kind is
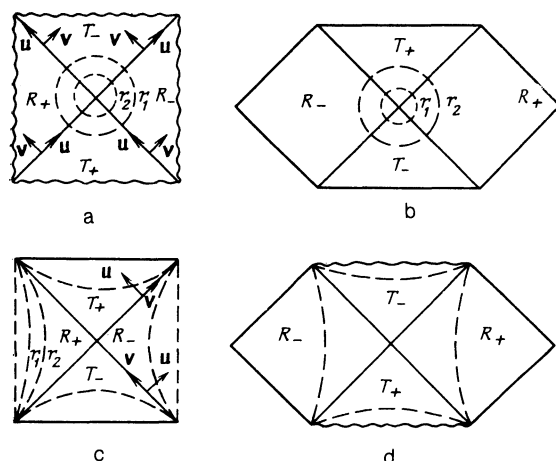


FIG. 3. Isotropic boundary between $R$ and $T$ regions: (a) $\alpha = 0$, $\beta > 0$; (b) $\alpha = 0$, $\beta < 0$; (c) $\beta = 0$, $\alpha > 0$, and (d) $\beta = 0$, $\alpha < 0$.

656    Sov. Phys. JETP **66** (4), October 1987

Berezin *et al.*    656

$$T_{\mu\nu}=\partial_\mu\varphi\partial_\nu\varphi-g_{\mu\nu}L+(\varepsilon+p)u_\mu u_\nu-g_{\mu\nu}p, \qquad (18)$$

where $\varphi$ is the scalar field strength, $L$ is its Lagrangian $L = 1/2(\partial_\mu\varphi)^2 - V$, $\varepsilon$ and $p$ are, respectively, the energy density and pressure in the ideal fluid in terms of comoving coordinates, and $u_\mu$ is the 4-velocity of the fluid, normalized by the condition $2u_\mu u_\nu/H = 1$.

In terms of the coordinates defined by (11),

$$T_v{}^u=\frac{1}{H}[(\partial_\nu\varphi)^2+(\varepsilon+p)(u_\nu)^2],$$

$$T_v{}^v=\frac{1}{2H}\partial_u\varphi\partial_\nu\varphi+V(\varphi)+\frac{\varepsilon-p}{2}. \qquad (19)$$

Consequently, in the system we are considering, we always have

$$\beta\geqslant 0, \qquad (20)$$

where $\beta = 0$, provided only $\varepsilon + p = 0$ and $\varphi_v = 0$. It can be shown, using the Einstein equation (9), that it also follows from these equations that $\varphi_u = 0$ and $dV/d\varphi = 0$, i.e., $\beta = 0$ corresponds to the pure vacuum case. Let us examine this case first.

## 1. Vacuum case

Suppose $\beta = 0$ throughout the space-time. When this holds, the component $T_v^v$ of the energy-momentum tensor is equal to a constant, i.e., the energy density of vacuum $\varepsilon_{vac}$. We therefore have

$$\alpha=\mathrm{sign}(8\pi\varkappa r^2\varepsilon_{vac}-1)|_{\Delta=0}. \qquad (21)$$

When $\varepsilon_{vac} = 0$, there is no dependence on $r$ in $\alpha$, and $\alpha = -1$. The complete vacuum diagram with $\varepsilon_{vac} = 0$ (i.e., the well-kown Penrose diagram for the Schwarzschild metric) is identical with that shown in Fig. 3d.

In general, on the other hand, Eq. (9) can readily be integrated in the vacuum case, $T_\mu^v = \varepsilon_{vac}\delta_\mu$:

$$\Delta=8\pi\varkappa r^2\varepsilon_{vac}/3+2\varkappa m/r-1, \qquad (22)$$

where $2\varkappa m$ is the constant of integration (from the boundary conditions and $m$ is the mass in the Schwarzschild metric). Suppose $m = 0$, $\varepsilon > 0$, in which case we have $r^2 = 3/8\pi\varkappa\varepsilon$ on the $\Delta = 0$ surface and $\alpha = \mathrm{sign}\, 2$. It follows that $\alpha$ does not then depend on $r$ and, being the diagram for the de Sitter universe, the complete diagram is identical with the diagram shown in Fig. 3c. When $m\neq 0$, $\varepsilon_{vac}\neq 0$, the equation $\Delta = 0$ can have two different real roots, two coincident roots, or no roots, where $\alpha$ assumes different values for different roots. The three corresponding Penrose diagrams are the successive combinations of certain parts of diagrams 3c and 3d. They are shown in Fig. 4.

## 2. Friedman universe

Now suppose that $\beta \neq 0$. We shall assume, for the sake of simplicity, that there is no scalar field in the system. In that case,

$$\alpha=\mathrm{sign}(4\pi\varkappa r^2(\varepsilon-p)-1)_{\Delta=0}. \qquad (23)$$

We shall also confine our attention to the isotropic homogeneous model. In terms of the corresponding coordinates (defined by the condition $u^0 = 1$), the Einstein equation (9) is readily integrated and yields $1 + \Delta = 8\pi\varkappa r^2\varepsilon/3$. Substituting this with $\Delta = 0$ in (23), we obtain
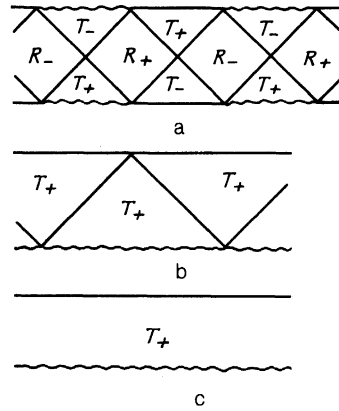


FIG. 4. Penrose diagrams for the Schwarzchild-de Sitter metric.

$$\alpha=\mathrm{sign}(\varepsilon-3p). \qquad (24)$$

This leads to the following classification of the types of $\Sigma$ surface: the $\Delta = 0$ surface is spacelike if $p > \varepsilon/3$, isotropic if $p = \varepsilon/3$, and timelike if $p < \varepsilon/3$.

The diagram of Fig. 5b thus corresponds to the closed Friedman universe $k = +1$) with $p = \varepsilon/3$. Only half of this diagram corresponds to the open model ($k = 0$, $k = -1$), where the diagonals must be associated with $r = \infty$ (Fig. 6b). Similarly, using the diagrams of Figs. 1a and b with $p > \varepsilon/3$, and Figs. 2a and b with $p < \varepsilon/3$, we can readily find the Penrose diagrams for all the possible configurations (summarized in Figs. 5 and 6).

## Chaotic inflation

Let us now suppose that there is a region of space-time with an approximately vacuum-type equation of state. Let us place the origin of coordinates at the center of this "fluctuation." Suppose that, at some instant of time, the size of this fluctuation becomes relatively large, i.e., it exceeds the corresponding Hubble radius, so that part of the "fluctuation" is located in the $T_+$ region. This situation can readily be imagined by considering that the "boundary" of the fluctuation cuts the $T_+$ region of diagram 3c, where, to the left of the boundary, the metric corresponds to Fig. 3c, while, to the right, it is arbitrary. We emphasize that the phrase "boundary of the fluctuation," is conventional because we are not using the thin-wall approximation at all. Instead, we can find the answer to a number of interesting questions by investigating the boundary between the $R$ and $T$ regions (which exists in the simple sense of this word), subject only to the large assumption that the fluctuation is sufficiently large for the $T_+$ region to be present in the manifold under consideration. We now ask: what is the possible environment of this fluctuation and, correspondingly, what should be its history?

The most trivial possibility corresponds to diagram 4c, in which the $T_+$ region occupies all space-time. However, this diagram does not correspond to the actually observed universe or the ideology of the inflationary scenario. We must therefore consider all the diagrams of Figs. 1–6 that contain the $T_+$ region, and this will readily lead us to the following conclusions.

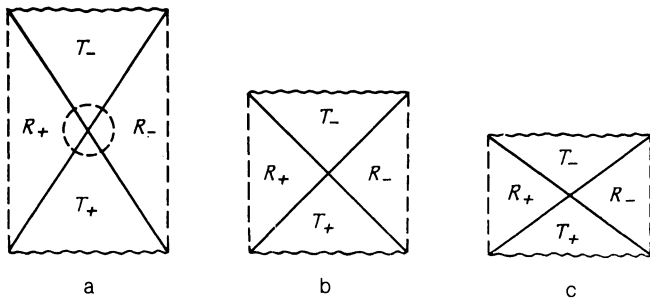All the diagrams corresponding to $\beta\geqslant 0$ are constructed so that the $T_+$ region extends either up to the maximum

FIG. 5. Closed Friedman universe: (a) $p < \varepsilon/3$, (b) $p = \varepsilon/3$, (c) $p > \varepsilon/3$.



FIG 6. Open Friedman universe: (a) $p < \varepsilon/3$, (b) $p = \varepsilon/3$, (c) $p > \varepsilon/3$.

possible values of $q$ ($T_+$ then lies lower than $T_-$) or the $R_-$ region lies to the right of $T_+$ (diagrams with $\beta < 0$ correspond to a state of matter that is unknown to us; in particular, this does not correspond to the system consisting of a perfect liquid and a scalar field). Hence, it follows immediately that an inflating fluctuation cannot be produced in a "laboratory."

However, these conditions in themselves do not impose a stringent enough limitation on the initial state of the Universe with an inflating fluctuation. Actually, the sufficient condition is that, at the initial time, the $T_+$ region extends right u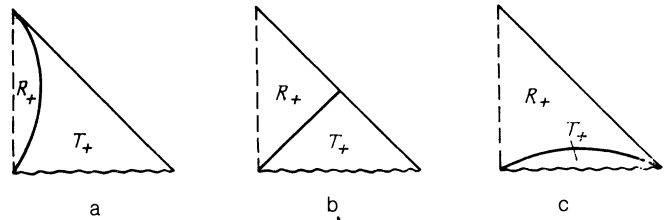p to the maximum possible values of $q$. This situation is not exceptional and occurs, for example, in the Friedman universe near a singularity.

[1] V. A. Berezin, V. A. Kuz'min, and I. I. Tkachev, Pis'ma Zh. Eksp. Teor. Fiz. **41**, 446 (1985) [JETP Lett. **41**, 547 (1985)]; V. A. Berezin, V. A. Kuzmin, and I. I. Tkachev, in Proc. Third Quantum Gravity Seminar, Moscow, October 1984, World Scientific, Singapore, 1985.

[2] E. Farhi and A. N. Guth, Phys. Lett. B **183**, 149 (1987).

[3] A. D. Linde, Pis'ma Zh. Eksp. Teor. Fiz. **38**, 149 (1983) [JETP Lett. **38**, 176 (1983)].

[4] I. D. Novikov, Soobshch. GAISh 132, No. 3, 43 (1964).

[5] L. D. Landau and E. M. Lifshitz, *The Classical Theory of Fields*, Pergamon Press, Oxford, 1971 (Russ. original, Nauka, Moscow, 1967].

Translated by S. Chomet